remote sensing

MDPI

Technical Note

Enhanced Warming in Global Dryland Lakes and Its Drivers

Siyi Wang [1], Yongli He [1,2,*], Shujuan Hu [1], Fei Ji [1], Bin Wang [3], Xiaodan Guan [1] and Sebastiano Piccolroaz [4,5]

1 Key Laboratory for Semi-Arid Climate Change of the Ministry of Education, College of Atmospheric Sciences, Lanzhou University, Lanzhou 730000, China; wangsy15@lzu.edu.cn (S.W.); hushuju@lzu.edu.cn (S.H.); jif@lzu.edu.cn (F.J.); guanxd@lzu.edu.cn (X.G.)
2 Collaborative Innovation Center for Western Ecological Safety, Lanzhou 730000, China
3 Environmental Science Division, Oak Ridge National Laboratory, Oak Ridge, TN 37831, USA; wangb@ornl.gov
4 Department of Civil, Environmental and Mechanical Engineering, University of Trento, 38123 Trento, Italy; s.piccolroaz@unitn.it
5 Physics of Aquatic Systems Laboratory (APHYS)-Margaretha Kamprad Chair, École Polytechnique Fédérale de Laussane, CH-1015 Lausanne, Switzerland
* Correspondence: heyongli@lzu.edu.cn

Abstract: Lake surface water temperature (LSWT) is sensitive to climate change. Previous studies have found that LSWT warming is occurring on a global scale and is expected to continue in the future. Recently, new global LSWT data products have been generated using satellite remote sensing, which provides an inimitable opportunity to study the LSWT response to global warming. Based on the satellite observations, we found that the warming rate of global lakes is uneven, with apparent regional differences. Indeed, comparing the LSWT warming in different climate zones (from arid to humid), the lakes in drylands experienced more significant warming (0.28 °C decade^{-1}) than those in semi-humid and humid regions (0.19 °C decade^{-1}) during previous decades (1995–2016). By further quantifying the impact factors, it showed that the LSWT warming is attributed to air temperature (74.4%), evaporation (4.1%), wind (9.9%), cloudiness (4.3%), net shortwave (3.1%), and net longwave (4.0%) over the lake surface. Air temperature is the main driving force for the warming of most global lakes, so the first estimate quantification of future LSWT trends can be determined from air temperature projections. By the end of the 21st century, the summer air temperature would warm up to 1.0 °C (SSP1-2.6) and 6.3 °C (SSP5-8.5) over lakes, with a more significant warming trend over the dryland lakes. Combined with their higher warming sensitivity, the excess summer LSWT warming in drylands is expected to continue, which is of great significance because of their high relevance in these water-limited regions.

Keywords: lake surface water temperature; satellite data; air temperature; climate change; limnology

Citation: Wang, S.; He, Y.; Hu, S.; Ji, F.; Wang, B.; Guan, X.; Piccolroaz, S. Enhanced Warming in Global Dryland Lakes and Its Drivers. *Remote Sens.* **2022**, *14*, 86. https://doi.org/10.3390/rs14010086

Academic Editor: Hainan Gong

Received: 18 November 2021
Accepted: 20 December 2021
Published: 24 December 2021

1. Introduction

Lakes store about 87% of the Earth's liquid surface freshwater resources [1] and play a key role in local and regional socio-economic development [2–4]. Water temperature is an important physical parameter for determining lakes' ecological health and their sustaining services to human society. Lake water temperature affects a variety of aspects of limnic systems, among which the survival and distribution of aquatic organisms [5], the rates of chemical reactions [6], fisheries production [7], hydrological and biogeochemical processes [8,9], and thermal stratification, thus the vertical exchange of energy and dissolved substances along the water column [10,11]. Several recent studies have shown that lake water temperature, among other factors, is sensitive to climate change [8,12–15]. For this reason and thanks to the relatively easy access to these type of observations (partially boosted by the increasing availability of thermal infrared imagery from space-borne satellites), lake surface water temperature (LSWT), in particular, has mainly been used as an eloquent indicator of climate change.

A large fraction of global lakes are located in drylands, including arid and semi-arid regions where precipitation is scarce (mean annual precipitation lower than 600 mm) [16,17], and the ecosystem is fragile. Lakes in drylands provide valuable ecosystem services and are a major source of water for human needs [18], yet drylands regions have experienced the most significant warming over the past century [19]. In the past few decades, dryland lakes have undergone tremendous changes in shape, size, and water level [20–22], making them particularly vulnerable to climate change. For example, the largest loss of global net permanent waters (over 70%) occurred in the Middle East and Central Asia, occupied mainly by drylands [23]. Recent evidence has shown that 34% of the lakes over the dry Mongolian Plateau have disappeared during the past three decades [24]. Climate change and human activities (i.e., agricultural irrigation) have been confirmed to be the main causes of the disappearance or shrinkage and dramatic water level variation of lakes in drylands [18,20,22,25]. Based on CMIP5 projections, drylands are expected to expand from 41% to 56% of global land area by the end of the 21st century under the RCP8.5 scenario due to surface energy allocation and radiation force of aerosol [26]. Therefore, lakes in drylands are speculated to be particularly threatened by global warming, and the number of lakes belonging to drylands regions is expected to increase in the future. While most of the published research on dryland lakes focused on changes in the lake area and water storage, relatively less attention has been given to understanding the climate controls on LSWT. The warming of LSWT is expected to affect several physical, chemical, and biological processes in lakes, with consequences for their aquatic ecosystem and associated ecosystem services. These are hot issues in today's research, which become particularly relevant when fragile dryland environments are considered.

Both in situ and satellite data indicate that global lakes have experienced a significant warming trend in recent decades, especially in summer [27,28]. However, the warming rate of lakes varies widely around the world [15,27]. In this respect, a recent reconstruction of LSWT during the past 20th century highlighted the fact that lakes have different sensitivity to climate change depending on the climatic zone in which they are located, lakes in the temperate region being the most sensitive [12]. Many studies on the dominant factors controlling LSWT response to climate change have been reported, however, most of them focused on lakes in specific regions, mainly in Europe and North America, while studies specifically focused on lakes in dryland regions are lacking. For example, the warming of LSWT is mainly caused by air temperature increase according to the LSWT predicted by six climate models on a global scale [29] and results of the Laurentian Great Lakes [30]. Schmid and Köster (2016) showed that 60% of the lake's warming is caused by increased air temperature and 40% by increased solar radiation for the Lower Lake Zurich [31]. Fink et al. (2014) found that increased absorption of solar radiation and long-wave radiation significantly enhanced the current warming rate in Lake Constance in Central Europe [32]. The increase in solar radiation and the decrease in near-surface wind speed played important roles in the increase of LSWT during the 2018 European heatwave [33]. Different reasons have been proposed to explain why LSWT is warming faster than the air temperature in some lakes, including lake thermal stratification [30], lake depth [34,35], water clarity [36], rivers inflow [32], humidity [31], and ice cover [27].

Despite the general advancements in understanding LSWT dynamics, specific research focused on the processes contributing to the LSWT response to global warming over the dryland regions remains limited. Recently, new LSWT data products were generated, e.g., GloboLakes [37], Global Lake Temperature Collaboration (GLTC) [28], and ARC-Lake (Paris, France) [38], offering a unique opportunity to investigate the response of LSWT at the global scale, with a specific focus on dryland regions. Based on the analysis of these datasets, we aimed to draw a better picture of the main meteorological drivers affecting dryland lakes' thermal dynamics. Specifically, we will address the following questions: (1) How did LSWT in different climate zones respond to global warming in the last decades? (2) What are the factors driving the response of dryland lake warming? (3) How LSWT is expected to evolve in the next century across the globe? Addressing these questions

poses the basis for future studies to evaluate how the expected global warming may affect dryland lakes in terms of water quality and aquatic ecosystem health.

2. Materials and Methods

2.1. Lake Surface Water Temperatures (LSWT) Data

Observed LSWTs were obtained from two data sets: GloboLakes LSWT v4.0 from satellite observations [37] and GLTC [28]. The GloboLakes dataset is available at http://www.laketemp.net (accessed on 30 April 2020), and was derived from the AVHRR on MetOpA, from the AATSR on Envisat, and the ATSR-2 on ERS-2 [37]. For the GloboLakes dataset, daily time series of satellite-derived LSWT for the period 1995–2016 were available for 979 lakes across the globe with a spatial resolution of 0.05°, from which we calculated the lake-average LSWT. Each LSWT pixel has a quality level index ranging from low (0) to best quality (5). In order to discard bad quality measurements, we computed the lake-average LSWT only using pixels with a quality index larger than 4, indicating the acceptable and best quality.

The GLTC dataset was compiled from in situ and satellite measurements by Sharma et al. (2015) [28], and consists of mean summer lake-averaged LSWTs from 291 lakes worldwide from 1985 to 2009. For lakes located in the Northern Hemisphere, summer was defined as July–September (JAS), whereas in the Southern Hemisphere, it was defined as January-March (JFM) [27,28,39]. In order to avoid the cloudy wet season of tropical climates and justified by the fact that in the tropical regions the air temperature range is very limited (absence of the traditional four thermal seasons), the JFM mean was used at latitudes between the equator and 23.5°N, and the JAS mean for latitudes between the equator and 23.5°S. This is consistent with the very minor air temperature range of tropical climates. The same summer season convention was used to compute the mean summer LSWT for the GloboLakes dataset.

2.2. Meteorological Data

Monthly mean precipitation, air temperature, evaporation, net shortwave, net longwave, wind, and cloudiness data at a spatial resolution of 0.25° were extracted from the ERA5 reanalysis datasets for the period 1995–2016 [40], consistently with that of the available LSWT observations. These data were used for climate classification and for investigating the dominant factors controlling LSWT in lakes belonging to different climate zones.

Daily air temperature from 9 different models of the sixth phase of Coupled Model Intercomparison Project (CMIP6) was also extracted and used to predict future air temperature changes. The 9 models considered here were identified based on data availability (detailed information is provided in Table S1 of the Supplementary Information). The scenario experiment of CMIP6 is a rectangular combination of the different shared socioeconomic pathway (SSP) and representative concentration pathway (RCP), which respectively represent the future global development and future climate radiative forcing level [41]. Two scenarios (SSP1-2.6 and SSP5-8.5) are used to analyze the low-force and high-force scenarios for future projections from 2015 to 2100. For a given SSPx-y scenario, x and y represent the specific SSP and RCP forcing pathways, respectively. Specifically, SSP1-2.6 represents the low end of the future forcing pathways spectrum and SSP5-8.5 represents the high edge of the future forcing pathways spectrum. SSP1-2.6 and SSP5-8.5 approximately correspond to RCP2.6 and RCP8.5, respectively [41]. In this paper, we choose the lowest and highest scenarios to maximize the range of future LSWT variability as much as possible, although the future is likely well beyond the SSP1-2.6 scenario at current emission rates. For both ERA5 and CMIP6 datasets, the climate variables corresponding to the analyzed lakes were extracted by identifying the closest grid point to the center of each lake [35]. When the elevation of the lake and the model grid is not the same, the lapse rate (Γ) was used to correct the surface air temperature to the over-lake value [12,42].

2.3. Climate Regionalization

The analysis of the ERA5 reanalysis dataset allowed to identify four climate zones depending on precipitation characteristics, including arid regions (mean annual precipitation—AP <200 mm yr^{-1}), semi-arid regions (200 $\leq$ AP < 600 mm yr^{-1}), semi-humid regions (600 $\leq$ AP < 1000 mm yr^{-1}) and humid regions (AP $\geq$ 1000 mm yr^{-1}) [16,17,43]. In the following, arid and semi-arid regions together are defined as drylands [16,43].

2.4. Warming Efficiency

Warming efficiency η is a simple lake-averaged indicator introduced by Toffolon et al. (2020) [44], which quantifies to what extent *LSWT* changes relative to a change in air temperature. In order to compute this indicator, first, the five coldest and five warmest years in the period 1995–2016 were identified (in terms of mean summer *LSWT*) for each lake. Then, the mean summer air temperature and *LSWT* from these years were averaged, obtaining values of mean air temperature and LSWT representative of the coldest ($\overline{AT}_{cold}$ and $\overline{LSWT}_{cold}$) and warmest years ($\overline{AT}_{warm}$ and $\overline{LSWT}_{warm}$, where the overbar indicates averaging over the corresponding five years). These averaged values were used to calculate the temperature difference between the warmest and coldest years, for both air temperature ($\Delta AT = \overline{AT}_{warm} - \overline{AT}_{cold}$) and *LSWT* ($\Delta LSWT = \overline{LSWT}_{warm} - \overline{LSWT}_{cold}$). Finally, the summer warming efficiency η was obtained as the ratio between the difference in *LSWT* and the difference in air temperature:

$$\eta = \frac{\Delta LSWT}{\Delta AT} \tag{1}$$

We first computed the warming efficiency of each lake, and then we determined the statistics for the four climate zones.

2.5. Attribution of LSWT Warming Trend

Previous studies identified six climate variables, including air temperature, evaporation, net shortwave, net longwave, wind and cloudiness, as the most important factors influencing *LSWT* [29–31,33,45]. In this study, a multiple linear regression model [46] was used to assess the relationship between summer *LSWT* and different climate variables. For the generic lake, the multiple linear regression model reads as

$$y = \beta_0 + \sum_{j=1}^{6} x_j \beta_j \tag{2}$$

where y is the vector of observed *LSWT* in summer for one lake of the GloboLakes dataset in the period 1995–2016 (y_i, with $i = 1, \ldots, 22$), x is the matrix of the six climate regressors ($x_{j,i}$, with $i = 1, \ldots, 22$ and $j = 1, \ldots, 6$) including air temperature, evaporation, net shortwave, net longwave, wind and cloudiness, and β_0, β_j, with $j = 1, \ldots, 6$ are unknown coefficients to be estimated through ordinary least squares (OLS) regression.

The total variance of summer *LSWT* explained by the six regressors taken together was quantified by the coefficient of determination R^2 of the full multiple linear model. Parallel to this, the relative contribution of each climate variable was estimated as the variable-specific R^2 contribution to the overall model R^2. The multiple linear regression analysis was performed using the Python package Pingouin version 0.3.8. Finally, the Theil-Sen estimator [47] was used to quantify the trends of *LSWT* and air temperature. Theil-Sen slope estimation is a nonparametric regression obtained by calculating the median pairwise slope combined with the median between two datasets. It avoids the effects of missing time series data and the shape of data distribution on the analysis results, and can exclude the interference of outliers in the time series.

3. Results

3.1. The Enhanced LSWT Warming in Drylands

The time series and global distribution of summer LSWT anomalies calculated relative to the climatology values during the overlapping period 1995–2005 for both GloboLakes and GLTC datasets are shown in Figure 1. The mean warming trend of summer LSWT from the two datasets are 0.39 °C decade^{-1} (95% CI: 0.35–0.43) and 0.25 °C decade^{-1} (95% CI: 0.23–0.26) across GLTC and GloboLakes datasets, respectively. Although there is interannual variability of summer LSWT, the warming trend of lakes is widespread distributed, which is consistent with previous studies [12,15,27]. However, the trends in summer LSWT for individual lakes range from -0.19 to 0.75 °C decade^{-1} (GloboLakes, Figure 1b) and from −0.12 to 0.87 °C decade^{-1} (GLTC, Figure 1c) (the 5th and 95th percentiles). Lakes in northwestern North America and central Europe are warming significantly faster than the global average (Figure 1b,c) [27]. In contrast, low-latitude (<23.5°) lakes typically experience a negative LSWT trend. Moreover, the warming rates in these lakes are heterogeneous even within the same region.

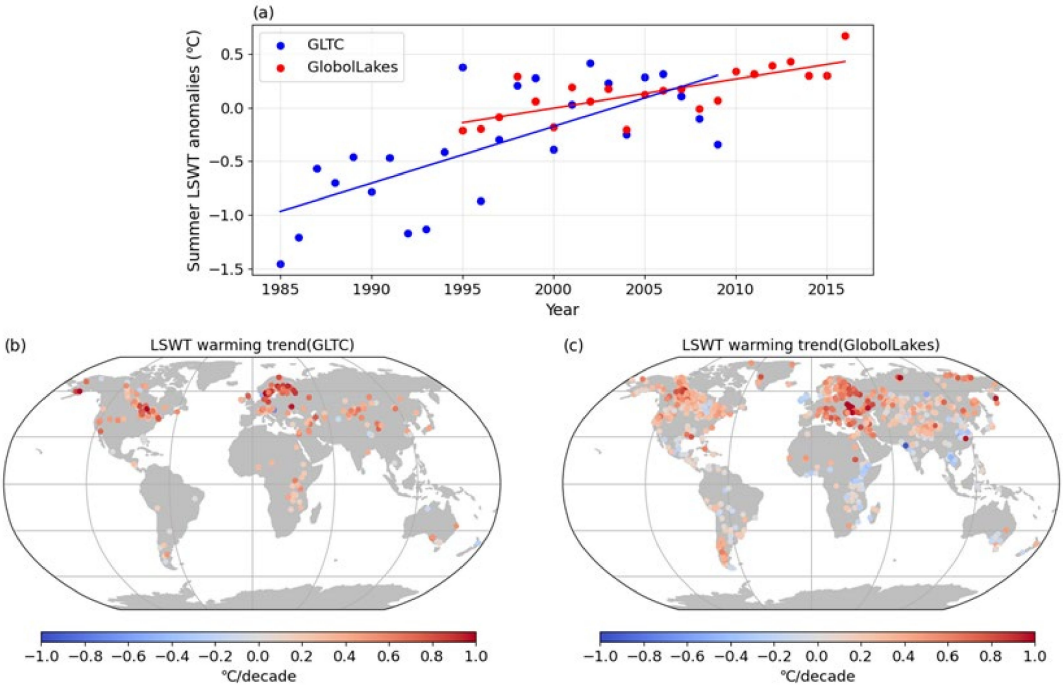

Figure 1. (**a**) Time series of summer mean lake surface water temperature (LSWT) anomalies at global scale based on GloboLakes (red) and Global Lake Temperature Collaboration (GLTC) (blue) datasets. The anomalies were calculated relative to the baseline period 1995–2005. The spatial distribution of summer LSWT trends for GLTC (**b**) and GloboLakes (**c**) datasets is also shown.

We classified climate zones as humid, semi-humid, semi-arid, and arid regions by precipitation (Figure 2a) as described in Section 2.3, and compared the trends of LSWT and air temperature in the four climate zones (Figure 2b,d). The air temperature was generally warming during 1995–2016, excluding weak negative trends in northeast North America, the middle of South America, some regions in Africa and Asia (Figure 2b). Considering the location of lakes (hereafter, for the sake of consistency, only the GloboLakes dataset is analyzed), it was found that these are generally distributed in areas where the air temperature increased. The abundance of lakes and the cumulative area they cover within each climate region make clear differences between climate regions (Figure 2c). The number of lakes in semi-arid regions is the largest, followed by semi-humid and humid regions, and the lakes in arid regions are the least. The largest cumulative area is in the humid and semi-humid regions. As a result, 49.6% of global lakes are located in drylands, assuming

homogeneous coverage of the GloboLakes dataset. As for the lake area, the largest coverage is found in the humid and semi-humid regions, indicating that the lakes in these regions have a larger individual surface area on average. Finally, Figure 2d compares the warming trends of LSWT with that of air temperature across the different climate zones. In general, comparing the warming of lakes in different climate zones shows that lakes in drylands are warming at a rate of 0.28 °C decade^{-1} in summer, which is about 50% faster than lakes in semi-humid and humid regions (0.19 °C decade^{-1}). Moreover, we notice that although air temperature warmed more in semi-humid regions than in other climate regions, lakes in semi-arid regions show the highest LSWT warming in summer.

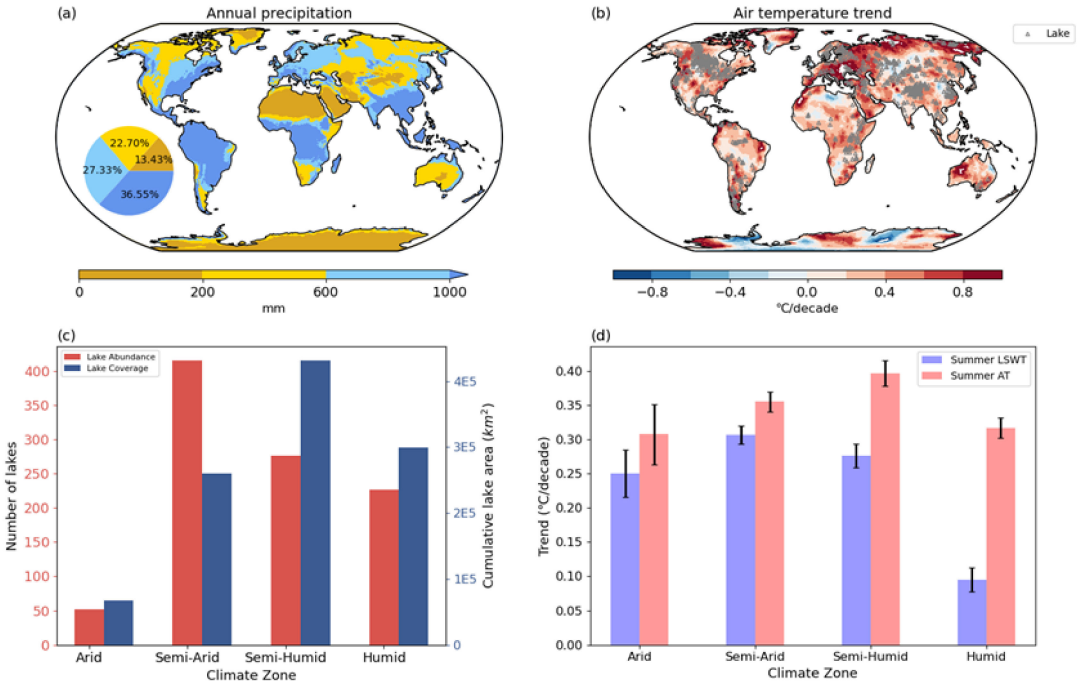

Figure 2. Global distribution of annually averaged precipitation (**a**) and air temperature trends (**b**) from ERA5 reanalysis between 1995 and 2016. The pie chart in (**a**) represents the percentage of land areas falling in the four climate zones. Gray triangles in (**b**) represent the locations of the global lakes (GloboLakes dataset). (**c**) The number and cumulative areas of lakes in different climate zones. (**d**) The mean warming trend of summer LSWT and air temperature in different climate zones. The error bars represent 1σ uncertainty.

More importantly, when computing the summer warming efficiency η, which effectively relates LSWT warming to the concurrent air temperature changes, lakes in the drylands region show the highest sensitivity to air temperature changes (Figure 3). Specifically, η in drylands is 1.18 on average (95% CI: 1.10–1.27), which is larger than 0.91 (95% CI: 0.85–0.98) of semi-humid lakes and 0.93 (95% CI: 0.87–1.00) of humid lakes (Figure 3b). It is interesting to note that the warming efficiency of lakes over the Qinghai-Tibet Plateau is much larger than that in other regions of the world (Figure 3). Overall, these results indicate that summer LSWT in drylands experience enhanced warming compared to semi-humid and humid regions and suggest that under the perspective of a warming climate, dryland lakes may face more risks than other aquatic ecosystems.

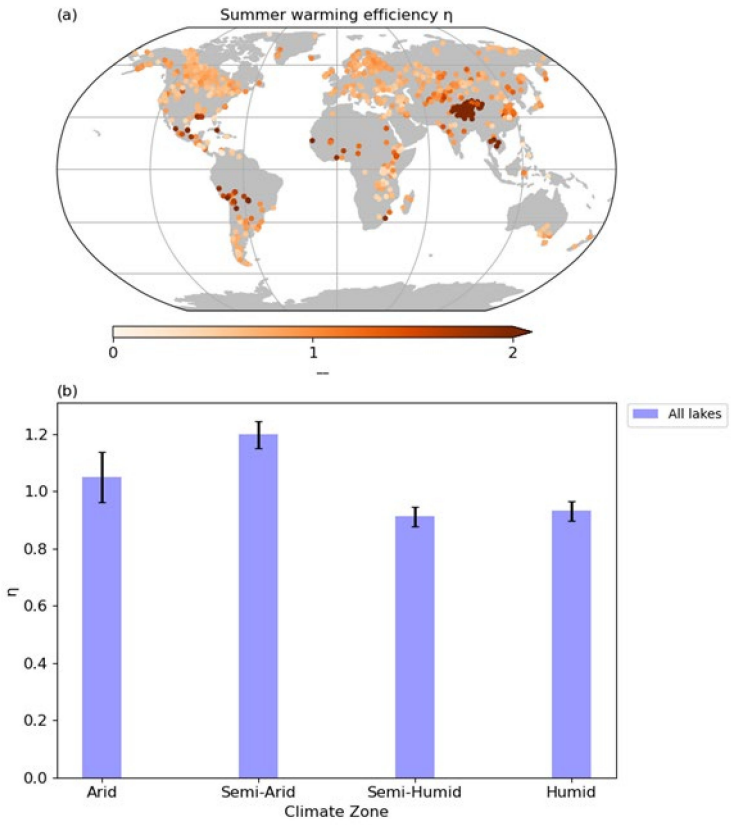

Figure 3. (**a**) Global spatial distribution of summer warming efficiency η of lakes during 1995–2016. (**b**) Mean warming efficiency of lakes in different climate zones. The error bars represent 1σ uncertainty.

3.2. The Drivers of Enhanced Dryland LSWT Warming

We quantify the relative contribution of air temperature, evaporation, net shortwave, net longwave, wind, and cloudiness to summer LSWT warming by multiple linear regression analysis (see Section 2.5). The full multiple linear regression model can explain about 0.64 (95% CI: 0.63–0.66) of the total summer LSWT variance (see overall model R^2 in Figure 4a), the total explained variance being slightly smaller for lakes in humid regions (R^2 = 0.52) than for lakes located in the other climate regions (mean R^2 = 0.66, Figure 4a). When looking at the relative contribution of each climate variable to the overall model R^2, air temperature is the most important factor to drive the response of summer LSWT in all the four climate zones (contributing to more than >40% of the total R^2). The wind is the second most important factor besides air temperature affecting LSWT in arid, semi-arid, and semi-humid regions, while it is the net longwave radiation in lakes located in humid zones, although wind speed is similarly important (Figure 4a). In any case, the five variables other than air temperature overall have similar effects on explaining summer LSWT, with relative contributions of about 10% to the total R^2. These results are confirmed when looking at the number of lakes where the different climate variables have been found to contribute the highest (Figure 4b,c) and at the spatial distribution of the most dominant factor around the world (Figure S1). Air temperature is the most important contributor in 74.4% of lakes on average (Figure 4b) and is the most prominent in the mid-high latitudes (Figures 4c and S1a). In the remaining 4.1%, 9.9%, 4.3%, 3.1%, and 4.0% of lakes, evaporation, wind, cloudiness, net shortwave, and longwave, respectively, are the dominant factor explaining summer LSWT variation. In general, the effect of wind is confirmed to be the second dominant factor after air temperature for lakes from arid to humid climate regions, with a hotspot concentrated in central North America. (Figure 4b,c). In any case, air temperature is the most dominant factor worldwide.

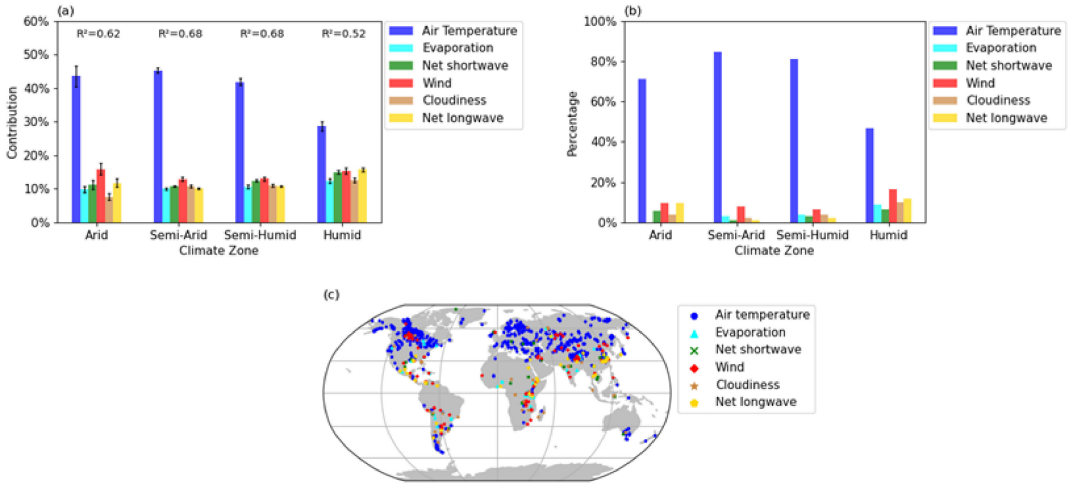

Figure 4. (**a**) R^2 of the full multiple linear model (text) and relative percentage contribution of the six climate variables across the four climate regions. The error bars represent 1σ uncertainty. (**b**) The percentage of lakes for each considered climate variable is the dominant factor in the full multiple linear model across the four climate regions. (**c**) Global distribution of the dominant climate variables to the full multiple linear model.

3.3. The Risk of Dryland LSWT Warming in the 21st Century

Based on the CMIP6 multi-model ensemble, mean summer air temperature at the GloboLakes locations is expected to increase at a comparable rate of about 0.42 °C/decade and 0.56 °C/decade globally under SSP1-2.6 and SSP5-8.5 scenarios during the period 2015–2040 (Figure 5a). After 2040, air temperature warming is expected to cease under the SSP1-2.6 scenario while continuing to rise at a higher rate of 0.81 °C/decade until the end of the 21st century under the SSP5-8.5 scenario. By the end of the 21st century, the summer air temperature over the global lakes is expected to warm up to 1.0 °C (SSP1-2.6) and 6.3 °C (SSP5-8.5), in the two cases.

As done for the historical period (Figure 2d), we analyzed the expected air temperature trend under the two future scenarios separating the different climate zones considered here. Compared with the other three climate regions, the expected air temperature trend in semi-arid regions is the highest under both scenarios, followed at a short distance by the warming trends in arid regions (Figure not shown). This implies that the air temperature warming rate in drylands (0.13 °C decade^{-1}, 0.80 °C decade^{-1}) is higher than that in semi-humid and humid regions (0.11 °C decade^{-1}, 0.65 °C decade^{-1}) under SSP1-2.6 and SSP5-8.5 scenario. This is particularly true under the SSP5-8.5 scenario (+23% excess warming in drylands compared to semi-humid and humid regions) than under the SSP1-2.6 scenario (+18%). Although the difference of air temperature warming between drylands and humid regions may be underestimated in the simulated results, all the considered CMIP6 models agree on projecting higher air temperature warming trends for dryland regions compared to humid and semi-humid regions (except for the EC-Earth3 and MPI-ESM1-2-LR models under SSP1-2.6, see Figure S2).

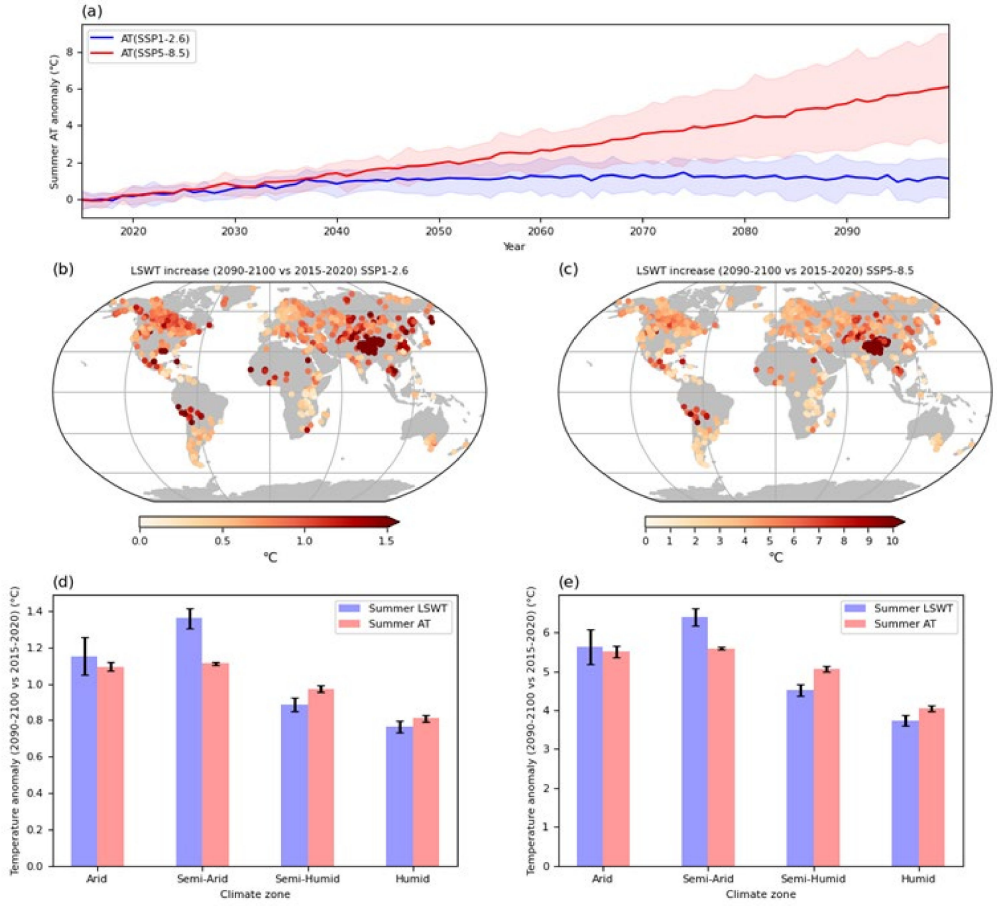

Figure 5. (**a**) Long-term time series of the multi-model ensemble mean summer air temperature anomalies for the lakes' locations in GloboLakes (lines), with the 5th to the 95th percentiles confidence interval (shaded areas) during 2015–2100. The anomalies were calculated relative to the baseline period 2015–2020. Multi-model ensemble mean warming (2090–2100 relative to 2015–2020) of summer LSWT across the different climate zones, under SSP1-2.6 scenario (**b**) and SSP5-8.5 scenario (**c**). The error bars represent 1σ uncertainty. The global spatial distribution of multi-model ensemble means summer LSWT and lakes' air temperature warming (2090–2100 relative to 2015–2020) under SSP1-2.6 (**d**) and SSP5-8.5 scenarios (**e**). The error bars represent 1σ uncertainty.

Because air temperature has been identified as the dominant driver of LSWT warming (Figure 4), the summer warming efficiency values found in Figure 3 can be used together with future air temperature trend obtained by each CMIP6 model to get the first estimate of the magnitude of LSWT warming until 2100. Specifically, the expected summer LSWT warming temperature has been calculated by multiplying the projected summer air temperature ($\Delta AT = \overline{AT}_{2090-2100} - \overline{AT}_{2015-2020}$) by the summer warming efficiency η for each lake and climate model. The worldwide spatial patterns of LSWT warming in 2090–2100 compared to 2015–2020 under the two considered scenarios are shown in Figure 5b–c. Under the SSP1-2.6 scenario, the mean LSWT is expected to increase to 1.08 °C (95% CI: 1.02–1.14 °C) (Figure 5b). Under the SSP5-8.5 scenario, the global lakes experience air temperature warming of 5.25 °C on average (95% CI: 5.01–5.48 °C) with some global lakes experiencing LSWT warming of more than 10 °C, with the fastest warming occurring in the Qinghai-Tibet Plateau and western South America around Peru and Bolivia (Figure 5c).

The results indicate that the existing warming trend of lakes in drylands will continue and will be higher than that in semi-humid and humid regions under both scenarios (Figure 5d,e). The warming of LSWT (2090–2100 compared to 2015–2020) in drylands (1.26 °C, 6.03 °C) is higher than that in semi-humid and humid regions (0.83 °C, 4.13 °C) under SSP1-2.6 and SSP5-8.5 scenarios, with a clear hotspot in the Qinghai-Tibet Plateau

confirming recent observations and model simulations [48]. The significant air temperature warming over lakes in arid and semi-arid regions enhanced by the higher warming sensitivity of these lakes will result in excess warming of dryland lakes compared to lakes in semi-humid and humid regions.

4. Discussion

The results presented here show that the global LSWTs increased significantly during 1995–2016 (Figure 1), confirming the conclusions of earlier studies [12,15,27,39,49]. Specifically, the present study provided an overview of the global distribution of LSWT warming separating among different climate zones defined based on precipitation statistics. Climate zone-specific analyses revealed consistent LSWT warming across the four climate zones, though the warming rate varied (Figure 2d). The analysis of the LSWT differences between the four climate zones showed higher LSWT warming in drylands compared to lakes in semi-humid and humid regions (Figure 2). This phenomenon is expected to continue in future scenarios based on the projected air temperature warming in the CMIP6 experiments.

LSWT warming is fundamentally determined by the imbalance of the lake surface energy budget, which is controlled by the heat flux terms in the heat energy budget, including incoming shortwave and longwave radiation, sensible and latent heat flux. Therefore, any factors that can affect these fluxes and hence the budget may drive LSWT warming, including cloud cover, over-lake wind speed, lake ice, and air temperature, for example, (i) Woolway et al. (2020) attributed the increase in LSWT to the disappearance of the ice sheet, evaporation, and changes in water volume, as well as mixing regimes [15], (ii) warming increases the importance of evaporation for the lake surface heat balance [29], and (iii) increased wind speed tends to cool down LSWT due to increased evaporation [50]. These processes interact with each other to influence the lake surface energy budget. Among these factors, air temperature, evaporation, and radiation are the most important drivers of LSWT warming [29,31,33,45]. Our analysis further identified air temperature as the most important factor worldwide, the other drivers being secondary regardless of climate region (Figure 4). However, wind speed is the second most important driver in all four climate regions (Figure 4), confirming its importance in affecting turbulent heat losses due to enhanced exchanges with the atmosphere and more intense wind-induced mixing.

We found that the differences in summer LSWT warming between drylands and humid regions are related to air temperature warming and lakes warming efficiency. First, drylands experienced a more enhanced air warming trend than humid areas in the historical period, which is mainly determined by the different responses of surface energy budget across the climate regions [26]. Indeed, the surface net energy in drylands prefers to allocate surface energy to sensible heat rather than latent heat due to the limitation of surface water resources. This mechanism has induced enhanced land and surface air warming in drylands, thus contributing to higher warming trends than humid regions. Second, the summer warming efficiency of lakes located in dryland is larger than that over the humid region, meaning that the dryland lakes are more sensitive to changes in air temperature. Moreover, warming efficiency is prominent in the Qinghai-Tibet Plateau. This suggests that besides the warming effect caused by concurrent higher air and land surface temperatures through conduction [51], previous meteorological conditions [44], the long ice-cover season lasting until April–May [52], and other physical processes such as albedo changes associated with snow/ice melting [53] or strong radiative warming penetrating the transparent ice cover [54] may contribute to higher warming efficiency, which deserves further investigation. Overall, the difference in the LSWT warming trend is combinedly caused by higher air temperature trends and warming efficiency in dryland lakes compared to lakes located in humid regions. Dryland lakes may face more risks than other aquatic ecosystems under the prospective warming climate.

Due to the projected enhanced dryland air temperature warming expected for the 21st century, the excess warming of LSWT in dryland lakes compared to lakes in humid regions

will continue in the future, which may seriously jeopardize their water quality, ecosystems, and even their future existence. It may also result in further shrinking and deterioration of precious dryland aquatic ecosystems. In fact, because of enhanced warming, lakes in drylands are drying up, especially the smallest ones such as the lakes on the Inner Mongolia plateau [24,55]. When these lakes shrink to the point of disappearing, the Bowen ratio (the ratio of sensible to latent heat) averaged in drylands will significantly increase due to the limitation of surface water available in the region, thus causing more surface energy to be allocated to sensible heat than latent heat and inducing an accelerated land and surface air temperature warming in dryland [43]. This creates positive feedback between air temperature warming on one side and LSWT warming and lake evaporation on the other, able to intensify the effects of climate change in these regions of the globe.

5. Conclusions

Lakes around the globe have experienced a significant warming trend in recent years. Dryland lakes, accounting for ~49.6% of the global lakes covered in this study, underwent a mean summer warming rate of 0.28 °C decade^{-1}, while a lower warming rate of 0.19 °C decade^{-1} characterized lakes in semi-humid and humid regions. The larger summer LSWT warming in drylands occurred irrespective of the fact that air temperature was increasing less than in semi-humid and humid regions and can be explained as resulting from higher thermal sensitivity of these lakes to changes in air temperature. Indeed, during the analyzed historical period (1995–2016), air temperature in drylands was warming 7% less than in semi-humid and humid regions, and the warming efficiency was 28% higher. The analysis of the historical data also confirmed previous findings indicating that air temperature is the dominant climatic factor controlling LSWT (in 74.4% of the studied lakes), while the other drivers have smaller and comparable importance. This suggests that the air temperature warming expected by the end of the 21st century is likely to have major consequences for LSWT. Indeed, the CMIP6 multi-model ensemble mean results indicate that the global summer air temperature warming can reach as high as 1.0 °C (SSP1-2.6) and 6.3 °C (SSP5-8.5) by the end of the century, with higher warming (18%/23%) expected in drylands. Considering the higher thermal sensitivity of lakes in this climate region, a first estimate quantification suggests that LSWT in drylands would continue to increase at higher rates (52%/46%) than LSWT in more humid regions.

Such excess warming of dryland lakes deserves further study, especially concerning a more detailed characterization of the possible positive feedback between air temperature warming and lake evaporation and shrinking in (progressively more) water-limited areas. Overall, LSWT warming in drylands is expected to raise serious concerns for the future state of these ecosystems, which may be particularly severe for communities living in arid regions where freshwater resources are of vital importance.

Supplementary Materials: The following supporting information can be downloaded at: https://www.mdpi.com/article/10.3390/rs14010086/s1, Figure S1: Relative contribution of air temperature (a), evaporation (b), net shortwave radiation (c), wind (d), cloudiness (e) and net longwave radiation (f) to the summer warming trend in global lakes; Figure S2: The summer air temperature trends of lakes in four climate zones under the SSP1-2.6 (a) and SSP5-8.5 (b) scenarios with 9 CMIP6 models. (c) Excess warming for each model under the SSP1-2.6 and SSP5-8.5 scenarios. Excess warming is calculated as (trend_drylands—trend_humidsemihumid)/trend_humidsemihumid*100. Table S1: List of 9 CMIP6 models in this study.

Author Contributions: Conceptualization, Y.H., S.H. and S.P.; methodology, Y.H., S.P. and S.W.; software, S.W.; validation, Y.H., S.H. and S.P.; formal analysis, Y.H., S.W. and S.P.; investigation, Y.H., S.W. and S.P.; resources, Y.H., S.H. and S.P.; data curation, S.W.; writing—original draft preparation, Y.H., S.W. and S.P.; writing—review and editing, S.H., F.J., B.W. and X.G.; visualization, S.P. and S.W.; supervision, Y.H., S.P. and S.H.; project administration, S.H.; funding acquisition, Y.H., S.H., F.J. and X.G. All authors have read and agreed to the published version of the manuscript.

Funding: This work was jointly supported by The National Key Research and Development Program of China (No: 2019YFA0607104), the National Science Foundation of China (42041004, 41775069, 41975076, 41521004, 41875083). This work was also supported by the Supercomputing Center of Lanzhou University.

Conflicts of Interest: The authors declare no conflict of interest.

References

1. Gleick, P.H. Water and conflict: Fresh water resources and international security. *Int. Secur.* **1993**, *18*, 79–112. [CrossRef]
2. Bai, J.; Chen, X.; Li, J.; Yang, L.; Fang, H. Changes in the area of inland lakes in arid regions of central Asia during the past 30 years. *Environ. Monit. Assess.* **2011**, *178*, 247–256. [CrossRef]
3. Fang, L.; Tao, S.; Zhu, J.; Liu, Y. Impacts of climate change and irrigation on lakes in arid northwest China. *J. Arid Environ.* **2018**, *154*, 34–39. [CrossRef]
4. Yapiyev, V.; Samarkhanov, K.; Tulegenova, N.; Jumassultanova, S.; Verhoef, A.; Saidaliyeva, Z.; Umirov, N.; Sagintayev, Z.; Namazbayeva, A. Estimation of water storage changes in small endorheic lakes in Northern Kazakhstan. *J. Arid Environ.* **2019**, *160*, 42–55. [CrossRef]
5. Lessard, J.L.; Hayes, D.B. Effects of elevated water temperature on fish and macroinvertebrate communities below small dams. *River Res. Appl.* **2003**, *19*, 721–732. [CrossRef]
6. Stumm, W.; Morgan, J.J. *Aquatic Chemistry: Chemical Equilibria and Rates in Natural Waters*; John Wiley & Sons: New York, NY, USA, 1996.
7. Ficke, A.D.; Myrick, C.A.; Hansen, L.J. Potential impacts of global climate change on freshwater fisheries. *Rev. Fish Biol. Fish.* **2007**, *17*, 581–613. [CrossRef]
8. Adrian, R.; O'Reilly, C.M.; Zagarese, H.; Baines, S.B.; Hessen, D.O.; Keller, W.; Livingstone, D.M.; Sommaruga, R.; Straile, D.; Van Donk, E. Lakes as sentinels of climate change. *Limnol. Oceanogr.* **2009**, *54*, 2283–2297. [CrossRef] [PubMed]
9. Jeppesen, E.; Meerhoff, M.; Davidson, T.A.; Trolle, D.; Sondergaard, M.; Lauridsen, T.L.; Beklioglu, M.; Brucet Balmaña, S.; Volta, P.; González-Bergonzoni, I.; et al. Climate change impacts on lakes: An integrated ecological perspective based on a multi-faceted approach, with special focus on shallow lakes. *J. Limnol.* **2014**, *73*, 88–111. [CrossRef]
10. Boehrer, B.; Schultze, M. Stratification of lakes. *Rev. Geophys.* **2008**, *46*. [CrossRef]
11. Kirillin, G.; Shatwell, T. Generalized scaling of seasonal thermal stratification in lakes. *Earth-Sci. Rev.* **2016**, *161*, 179–190. [CrossRef]
12. Piccolroaz, S.; Woolway, R.I.; Merchant, C.J. Global reconstruction of twentieth century lake surface water temperature reveals different warming trends depending on the climatic zone. *Clim. Chang.* **2020**, *160*, 427–442. [CrossRef]
13. Vinnå, L.R.; Medhaug, I.; Schmid, M.; Bouffard, D. The vulnerability of lakes to climate change along an altitudinal gradient. *Commun. Earth Environ.* **2021**, *2*, 35. [CrossRef]
14. Williamson, C.E.; Saros, J.E.; Vincent, W.F.; Smol, J.P. Lakes and reservoirs as sentinels, integrators, and regulators of climate change. *Limnol. Oceanogr.* **2009**, *54*, 2273–2282. [CrossRef]
15. Woolway, R.I.; Kraemer, B.M.; Lenters, J.D.; Merchant, C.J.; O'Reilly, C.M.; Sharma, S. Global lake responses to climate change. *Nat. Rev. Earth Environ.* **2020**, *1*, 388–403. [CrossRef]
16. Huang, J.; Guan, X.; Ji, F. Enhanced cold-season warming in semi-arid regions. *Atmos. Chem. Phys.* **2012**, *12*, 5391–5398. [CrossRef]
17. Thomas, D.; United Nations Environment Programme. *World Atlas of Desertification*; Arnold, E., Ed.; United Nations Environment Programme: London, UK, 1992; Volume 45. [CrossRef]
18. Liu, H.; Chen, Y.; Ye, Z.; Li, Y.; Zhang, Q. Recent lake area changes in central Asia. *Sci. Rep.* **2019**, *9*, 16277. [CrossRef]
19. Huang, J.; Li, Y.; Fu, C.; Chen, F.; Fu, Q.; Dai, A.; Shinoda, M.; Ma, Z.; Guo, W.; Li, Z. Dryland climate change: Recent progress and challenges. *Rev. Geophys.* **2017**, *55*, 719–778. [CrossRef]
20. Cao, Y.; Fu, C.; Wang, X.; Dong, L.; Yao, S.; Xue, B.; Wu, H.; Wu, H. Decoding the dramatic hundred-year water level variations of a typical great lake in semi-arid region of northeastern Asia. *Sci. Total Environ.* **2021**, *770*, 145353. [CrossRef]
21. Fu, C.; Wu, H.; Zhu, Z.; Song, C.; Xue, B.; Wu, H.; Ji, Z.; Dong, L. Exploring the potential factors on the striking water level variation of the two largest semi-arid-region lakes in northeastern Asia. *Catena* **2021**, *198*, 105037. [CrossRef]
22. Tan, C.; Guo, B.; Kuang, H.; Yang, H.; Ma, M. Lake area changes and their influence on factors in arid and semi-arid regions along the silk road. *Remote Sens.* **2018**, *10*, 595. [CrossRef]
23. Pekel, J.-F.; Cottam, A.; Gorelick, N.; Belward, A.S. High-resolution mapping of global surface water and its long-term changes. *Nature* **2016**, *540*, 418–422. [CrossRef] [PubMed]
24. Tao, S.; Fang, J.; Zhao, X.; Zhao, S.; Shen, H.; Hu, H.; Tang, Z.; Wang, Z.; Guo, Q. Rapid loss of lakes on the Mongolian Plateau. *Proc. Natl. Acad. Sci. USA* **2015**, *112*, 2281–2286. [CrossRef]
25. Zhang, G.; Yao, T.; Chen, W.; Zheng, G.; Shum, C.; Yang, K.; Piao, S.; Sheng, Y.; Yi, S.; Li, J. Regional differences of lake evolution across China during 1960s–2015 and its natural and anthropogenic causes. *Remote Sens. Environ.* **2019**, *221*, 386–404. [CrossRef]
26. Huang, J.; Yu, H.; Guan, X.; Wang, G.; Guo, R. Accelerated dryland expansion under climate change. *Nat. Clim. Chang.* **2016**, *6*, 166–171. [CrossRef]

27. O'Reilly, C.M.; Sharma, S.; Gray, D.K.; Hampton, S.E.; Read, J.S.; Rowley, R.J.; Schneider, P.; Lenters, J.D.; McIntyre, P.B.; Kraemer, B.M.; et al. Rapid and highly variable warming of lake surface waters around the globe. *Geophys. Res. Lett.* **2015**, *42*, 10773–10781. [CrossRef]
28. Sharma, S.; Gray, D.K.; Read, J.S.; O'Reilly, C.M.; Schneider, P.; Qudrat, A.; Gries, C.; Stefanoff, S.; Hampton, S.E.; Hook, S.; et al. A global database of lake surface temperatures collected by in situ and satellite methods from 1985–2009. *Sci. Data* **2015**, *2*, 150008. [CrossRef] [PubMed]
29. Schmid, M.; Hunziker, S.; Wüest, A. Lake surface temperatures in a changing climate: A global sensitivity analysis. *Clim. Chang.* **2014**, *124*, 301–315. [CrossRef]
30. Zhong, Y.; Notaro, M.; Vavrus, S.J.; Foster, M.J. Recent accelerated warming of the Laurentian Great Lakes: Physical drivers. *Limnol. Oceanogr.* **2016**, *61*, 1762–1786. [CrossRef]
31. Schmid, M.; Köster, O. Excess warming of a Central European lake driven by solar brightening. *Water Resour. Res.* **2016**, *52*, 8103–8116. [CrossRef]
32. Fink, G.; Schmid, M.; Wahl, B.; Wolf, T.; Wüest, A. Heat flux modifications related to climate-induced warming of large European lakes. *Water Resour. Res.* **2014**, *50*, 2072–2085. [CrossRef]
33. Woolway, R.I.; Jennings, E.; Carrea, L. Impact of the 2018 European heatwave on lake surface water temperature. *Inland Waters* **2020**, *10*, 322–332. [CrossRef]
34. Calamita, E.; Piccolroaz, S.; Majone, B.; Toffolon, M. On the role of local depth and latitude on surface warming heterogeneity in the Laurentian Great Lakes. *Inland Waters* **2021**, *11*, 208–222. [CrossRef]
35. Woolway, R.I.; Merchant, C.J. Amplified surface temperature response of cold, deep lakes to inter-annual air temperature variability. *Sci. Rep.* **2017**, *7*, 4130. [CrossRef] [PubMed]
36. Rose, K.C.; Winslow, L.A.; Read, J.S.; Hansen, G.J.A. Climate-induced warming of lakes can be either amplified or suppressed by trends in water clarity. *Limnol. Oceanogr. Lett.* **2016**, *1*, 44–53. [CrossRef]
37. Carrea, L.; Merchant, C. GloboLakes: Lake Surface Water Temperature (LSWT) v4.0 (1995–2016). *Cent. Environ. Data Anal.* **2019**. [CrossRef]
38. MacCallum, S.N.; Merchant, C.J. Surface water temperature observations of large lakes by optimal estimation. *Can. J. Remote Sens.* **2012**, *38*, 25–45. [CrossRef]
39. Schneider, P.; Hook, S.J. Space observations of inland water bodies show rapid surface warming since 1985. *Geophys. Res. Lett.* **2010**, *37*, L22405. [CrossRef]
40. Hersbach, H.; Bell, B.; Berrisford, P.; Biavati, G.; Horányi, A.; Muñoz Sabater, J.; Nicolas, J.; Peubey, C.; Radu, R.; Rozum, I.; et al. ERA5 Monthly Averaged Data on Single Levels from 1979 to Present Copernicus Climate Change Service (C3S) Climate Data Store (CDS). 2019. Available online: https://cds.climate.copernicus.eu/cdsapp#!/dataset/reanalysis-era5-single-levels-monthly-means?tab=overview (accessed on 1 June 2020). [CrossRef]
41. Fan, X.; Duan, Q.; Shen, C.; Wu, Y.; Xing, C. Global surface air temperatures in CMIP6: Historical performance and future changes. *Environ. Res. Lett.* **2020**, *15*, 104056. [CrossRef]
42. Gao, L.; Bernhardt, M.; Schulz, K. Elevation correction of ERA-Interim temperature data in complex terrain. *Hydrol. Earth Syst. Sci.* **2012**, *16*, 4661–4673. [CrossRef]
43. Huang, J.; Yu, H.; Dai, A.; Wei, Y.; Kang, L. Drylands face potential threat under 2 C global warming target. *Nat. Clim. Chang.* **2017**, *7*, 417–422. [CrossRef]
44. Toffolon, M.; Piccolroaz, S.; Calamita, E. On the use of averaged indicators to assess lakes' thermal response to changes in climatic conditions. *Environ. Res. Lett.* **2020**, *15*, 034060. [CrossRef]
45. Winslow, L.A.; Leach, T.H.; Rose, K.C. Global lake response to the recent warming hiatus. *Environ. Res. Lett.* **2018**, *13*, 054005. [CrossRef]
46. Grömping, U. Relative importance for linear regression in R: The package relaimpo. *J. Stat. Softw.* **2006**, *17*, 1–27. [CrossRef]
47. Sen, P.K. Estimates of the Regression Coefficient Based on Kendall's Tau. *J. Am. Stat. Assoc.* **1968**, *63*, 1379–1389. [CrossRef]
48. Huang, L.; Wang, J.; Zhu, L.; Ju, J.; Daut, G. The warming of large lakes on the Tibetan Plateau: Evidence from a lake model simulation of Nam Co, China, during 1979–2012. *J. Geophys. Res.* **2017**, *122*, 13095–13107. [CrossRef]
49. Austin, J.A.; Colman, S.M. Lake Superior summer water temperatures are increasing more rapidly than regional air temperatures: A positive ice-albedo feedback. *Geophys. Res. Lett.* **2007**, *34*, L06604. [CrossRef]
50. Valerio, G.; Pilotti, M.; Barontini, S.; Leoni, B. Sensitivity of the multiannual thermal dynamics of a deep pre-alpine lake to climatic change. *Hydrol. Process.* **2015**, *29*, 767–779. [CrossRef]
51. Zhang, G.; Yao, T.; Xie, H.; Yang, K.; Zhu, L.; Shum, C.; Bolch, T.; Yi, S.; Allen, S.; Jiang, L. Response of Tibetan Plateau's lakes to climate changes: Trend, pattern, and mechanisms. *Earth-Sci. Rev.* **2020**, *208*, 103269. [CrossRef]
52. Kropáček, J.; Maussion, F.; Chen, F.; Hoerz, S.; Hochschild, V. Analysis of ice phenology of lakes on the Tibetan Plateau from MODIS data. *Cryosphere* **2013**, *7*, 287–301. [CrossRef]
53. Ghatak, D.; Sinsky, E.; Miller, J. Role of snow-albedo feedback in higher elevation warming over the Himalayas, Tibetan Plateau and Central Asia. *Environ. Res. Lett.* **2014**, *9*, 114008. [CrossRef]

54. Kirillin, G.B.; Shatwell, T.; Wen, L. Ice-Covered Lakes of Tibetan Plateau as Solar Heat Collectors. *Geophys. Res. Lett.* **2021**, *48*, e2021GL093429. [CrossRef]
55. Zhang, G.; Yao, T.; Piao, S.; Bolch, T.; Xie, H.; Chen, D.; Gao, Y.; O'Reilly, C.M.; Shum, C.; Yang, K. Extensive and drastically different alpine lake changes on Asia's high plateaus during the past four decades. *Geophys. Res. Lett.* **2017**, *44*, 252–260. [CrossRef]